FORMABILITY OF SUPERPLASTIC DEEP DRAWING PROCESS WITH MOVING BLANK HOLDER FOR AA1050-H18 CONICAL CUPS

A. Chennakesava Reddy[1]

[1]*Professor, Department of Mechanical Engineering, JNT University, Hyderabad-500 085, India*

Abstract

In this present work, a statistical approach based on Taguchi Techniques and finite element analysis were adopted to determine the formability of conical cup using warm deep drawing process. The process parameters were temperature, coefficient of friction, strain rate and blank holder velocity. The experimental results were validated using a finite element software namely D-FORM. The AA1050–H18 sheets were used for the superplastic deep drawing of the conical cups. The strain rate by itself has a significant effect on the effective stress and the height of the conical cup drawn. The formability of the conical cups was outstanding for the surface expansion ratio greater than 2.0.

Keywords: *AA1050-H18, superplastic deep drawing, blank holder velocity, temperature, coefficient of friction, strain rate, conical cups, formability.*

----------***----------

1. INTRODUCTION

The deep drawing process is a forming process which occurs under a combination of tensile and compressive conditions. When drawing complex products in practice, there is usually a combination of stretch and deep drawing involved. Common deep drawn products are cans, boxes, and bottles, as well as irregularly shaped products. Parts produced by hot forming are characterized by high strength, complex shapes.

Superplasticity consists in the ability of some materials to develop very large tensile elongations without necking. Material requirements for structural superplasticity are fine and equiaxed microstructure (grain size generally < 10 μm), grains stable under high temperature, temperature high than 0.4 Tm (absolute melting point) and strain rate sensitivity exponent > 0.3 [1]. The formability limitations of deep drawing are a barrier for some industrial uses. At too a strain rate the blank lack of ductility while at too low a strain rat it fails from lack of strength. Radial drawing stress and tangential compressive stress are a common concern that can result in wrinkling, fracturing or cracking in some applications. The process variables, which affect the failure of the cup drawing process, include material properties, die design, and process parameters such as temperature, coefficient of friction, strain rate, blank holding force, punch and die corner radii and drawing ratio [2, 3, 4]. The ductility of common aluminum alloys increases with temperature. Thus forming at elevated temperatures close to the recrystallization temperature of about 300 °C, also called warm forming, is one of the promising methods to improve formability. The deep drawing process of an aluminum alloy has been simulated to study the deformation behavior and the temperature change and successfully predicted the forming limit and necking site by comparing the numerical results with experimental results [5]. In a research on low carbon steel, the results conclude that with enhancement of strain rate and reduction of temperature, the tensile strength increases and entire flow curve of material increases its level [6]. Friction is another important parameter that influences the deep drawing process. In metal forming processes, the friction influences the strain distribution at tool blank interface and drawability of metal sheet. In the experimental work carried out on the warm deep drawing process of the EDD steel it has been observed that the extent of thinning at punch corner radius is found to be lesser in the warm deep-cup drawing process of extra-deep drawing (EDD) steel at 200^0C [7]. In another work performed by the author [8] on the cup drawing process using an implicit finite element analysis, the thinning is observed on the vertical walls of the cup with high values of strain at the thinner sections. In the finite element simulations, a forming limit diagram (FLD) has been successfully applied to analyze the fracture phenomena by comparing the strain status [9].

AA1050 is known for its excellent corrosion resistance, high ductility and highly reflective finish. Applications of AA1050 are typically used for chemical process plant equipment, food industry containers, architectural flashings, lamp reflectors, and cable sheathing. AA1050 aluminum alloy is not heat treatable. It is difficult to deep draw and to have minimum wall thickness of less than 1 mm. Therefore, it is expensive to exploit the combination of high strength and thin wall cups using deep drawing process.

In the present work, the formability of warm deep drawing process was assessed during the fabrication of AA1050-H18 conical cups. The investigation was focused on the process parameters such as temperature, coefficient of friction, strain rate and blank holder velocity at constant force. The design of experiments was carried out using Taguchi technique and the warm deep drawing process was executed using the finite element analysis software namely D-FORM 3D.

2. MATERIALS AND METHODS

AA1050-H18 was used to fabricate conical cups. The levels chosen for the control parameters were in the operational range of AA1050-H18 aluminum alloy using deep drawing process. Each of the three control parameters was studied at three levels. The chosen control parameters are summarized in table 1. The orthogonal array (OA), L9 was selected for the present work. The parameters were assigned to the various columns of O.A. The assignment of parameters along with the OA matrix is given in table 2.

Table-1: Control parameters and levels

Factor	Symbol	Level–1	Level–2	Level–3
Temperature, ^{0}C	A	300	400	500
Strain rate, 1/s	B	10	20	30
Coefficient of friction	C	0.05	0.075	0.1
BH velocity, mm/s	D	0.5	0.6	0.7

Table-2: Orthogonal array (L9) and control parameters

Treat No.	A	B	C	D
1	1	1	1	1
2	1	2	2	2
3	1	3	3	3
4	2	1	2	3
5	2	2	3	1
6	2	3	1	2
7	3	1	3	2
8	3	2	1	3
9	3	3	2	1

The blank size was calculated by equating the surface area of the finished drawn cup with the area of the blank. The blank diameter, d_b is given by:

$$d_b = \sqrt{{d_2}^2 + (d_1 + d_2)\sqrt{(d_1 - d_2)^2 + 4h^2}} \quad (1)$$

where $d_1$and d_2 are the top and bottom diameters of the cup and h is the height of the cup.

The top and bottom diameters of the punch are those of the cup. The height of the punch is that of the cup. The drawing punch must have corner radius exceeding three times the blank thickness (t). However, the punch radius should not exceed one-fourth the cup diameter (d). The punch radius is expressed as:

$$r_p = \frac{12t+d}{8} \quad (2)$$

For smooth material flow the die edge should have generous radius preferably four to six times the blank thickness but never less than three times the sheet thickness because lesser radius would hinder material flow while excess radius would reduce the pressure area between the blank and the blank holder. The corner radius of the die can be calculated from the following equation:

$$r_d = 0.8\sqrt{(D-d)t} \quad (3)$$

The material flow in drawing may render some flange thickening and thinning of walls of the cup inevitable. The space for drawing is kept bigger than the sheet thickness. This space is called die clearance.

$$\text{Clearance, } c_d = t \pm \mu\sqrt{10t} \quad (4)$$

where μ is the coefficient of friction.

The top diameter of the die is obtained from the following equation:

$$d_{d1} = d_1 + 2c_d \quad (5)$$

The bottom diameter of the die is obtained from the following equation:

$$d_{d2} = d_2 + 2c_d \quad (6)$$

The height of the die is the height of the cup.

3. FINITE ELEMENT MODELING AND ANALYSIS

The finite element modeling and analysis was carried using D-FORM 3D software. The conical sheet blank was created with desired diameter and thickness using CAD tools [10]. The conical top punch, conical bottom hollow die were also modeled with appropriate inner and outer radius and corner radius using CAD tools. The clearance between the punch and die was calculated as in Eq. (4). The sheet blank was meshed with tetrahedral elements [11]. The modeling parameters of deep drawing process were as follows:
Number of tetrahedron elements for the blank: 21980
Number of nodes for the blank: 7460
Number of polygons for top die: 9120
Number of polygons for bottom die: 9600

The basic equations of the rigid-plastic finite element analysis are as follows:

Equilibrium equation:

$$\sigma_{ij,j} = 0 \quad (7)$$

Compatibility and incompressibility equations:

$$\text{Strain rate tensor, } \dot{\varepsilon}_{ij} = \frac{1}{2}\left(u_{i,j} + u_{j,i}\right),\ \dot{\varepsilon}_{kk} = 0 \quad (8)$$

where $u_{i,j}$ and $u_{j,i}$ are velocity vectors.

Constitutive equations:

$$\text{Stress tensor, } \sigma_{ij} = \frac{2\sigma_{eq}}{3\varepsilon_{eq}}\dot{\varepsilon}_{ij} \quad (9)$$

where, equivalent stress, $\sigma_{eq} = \sqrt{\frac{3}{2}\left(\acute{\sigma_{ij}}, \acute{\sigma_{ij}}\right)}$ and equivalent strain, $\varepsilon_{eq} = \sqrt{\frac{3}{2}\left(\acute{\varepsilon_{ij}}\,\acute{\varepsilon_{ij}}\right)}$.

The Coulomb's friction model was given by

$$\tau_f = \mu p \quad (10)$$

where μ is the coefficient of friction (COF), p is the normal pressure, and τ_f is the frictional shear stress.

The flow stress based on the strain hardening is computed by the following equation:

$$\sigma_f = K\varepsilon^n \quad (11)$$

where, K and n are work hardening parameters depending on mechanical properties of material.

The flow stress equation considering the effects of the strain, strain rate and temperature is given by

$$\sigma_f = f\left(\varepsilon, \dot{\varepsilon}, T\right) \quad (12)$$

where, ε represents the strain, $\dot{\varepsilon}$ represents the strain rate and T represents the temperature.

Johnson-Cook Model [12] is among the most widely used mode. It connects all the deformation parameters in the following compact form.

$$\sigma_f = [\sigma + K\varepsilon^n]\left[1 + Sln\frac{\dot{\varepsilon}}{\dot{\varepsilon_0}}\right]\left[1 - \left(\frac{T-T_0}{T_m-T_0}\right)^m\right] \quad (13)$$

where, $\dot{\varepsilon_0}$ is a reference strain rate taken for normalization; σ is the yield stress and K is the strain hardening factor, whereas S is a dimensionless strain rate hardening coefficient. Parameters n and m are the power exponents of the effective strain and strain rate.

Hill's and Swift's theories used to calculate the forming limit strains on the left and the right side, respectively, of the forming limit diagram (FLD). Assuming that the strain-stress relationship of sheets can be expressed by Hollomon's equation the formulae calculating the forming limit strains can be written as follows, with stress ratio, $\alpha = \sigma_1/\sigma_2$.

For $\varepsilon_2 < 0$

$$\varepsilon_{l1} = \frac{1+(1-\alpha)r}{1+\alpha}n \quad (14)$$

$$\varepsilon_{l2} = \frac{\alpha+(1-\alpha)r}{1+\alpha}n \quad (15)$$

Normal anisotropy value represents the ratio of the natural width deformation in relation to the thickness deformation of a strip specimen elongated by uniaxial tensile stress:

$$r = \frac{\varepsilon_w}{\varepsilon_t} \quad (16)$$

For $\varepsilon_2 > 0$

$$\varepsilon_{l1} = \frac{(1+r_{0-r_0}\alpha)\left[1+r_0+\alpha^2\left(\frac{r_0}{r_{90}}\right)(1+r_{90})-2\alpha r_0\right]}{(1+r_0-r_0\alpha)^2+\alpha\left(\alpha\frac{r_0(1+r_{90})}{r_{90}}-r_0\right)^2}n \quad (17)$$

$$\varepsilon_{l2} = \frac{(1+r_{0-r_0}\alpha)\left[\alpha+\alpha r_0-\alpha^2 r_0+\alpha^2\left(\frac{r_0}{r_{90}}\right)(1+r_{90})-r_0\right]}{(1+r_0-r_0\alpha)^2+\alpha\left(\alpha\frac{r_0(1+r_{90})}{r_{90}}-r_0\right)^2}n \quad (18)$$

For plasticity studies, the basic definition of r-value has been replaced with the instantaneous r_i value, which is defined as

$$r_i = \frac{d\varepsilon_w}{d\varepsilon_t} \quad (19)$$

In the present work, the contact between blank/punch, blank/blank holder and die/blank were coupled as contact pair (figure 1). The mechanical interaction between the contact surfaces was assumed to be frictional contact and modeled as Coulomb's friction model as defined in Eq. (10). A constant force of 1000 N was applied on a moving blank holder. The time taken to complete the superplastic deep drawing was taken as 15 seconds. The distance to move the blank holder was calculated based on the predesigned velocity as per the design of experiments. The finite element analysis was chosen to find the metal flow, effective stress, height of the cup, and damage of the cup. The finite element analysis was carried out using D-FORM 3D software according to the design of experiments.

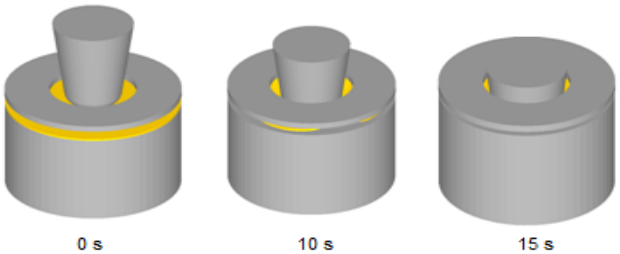

Fig-1: Conical cup drawing at different steps.

4. RESULTS AND DISCUSSION

Two trials were carried out with different meshes for each experiment. For the ANOVA (analysis of variance) the Fisher's test (F = 3.01) was carried out on all the parameters (A, B, C and D) at 90% confidence level.

4.1 Influence of Process Parameters on Effective Stress

Table 3 gives the ANOVA (analysis of variation) summary of the effective stress. The strain rate (B) by itself had a sub-

stantial effect (87.95%) on the effective stress. The temperature (A) had an effect of 7.15% on the effective stress. The coefficient of friction(C) and blank holder (BH) velocity (D) had contributed 2.66% and 2.13% of the total variation observed in the effective stress respectively.

Table-3: ANOVA summary of the effective stress

Source	Sum 1	Sum 2	Sum 3	*SS*	*v*	*V*	*F*	*P*
A	517.20	635.30	520.80	1503.93	2	751.97	65.96	7.15
B	809.00	521.90	342.40	18464.57	2	9232.29	809.85	87.95
C	517.90	555.50	599.90	561.61	2	280.81	24.63	2.66
D	600.20	535.60	537.50	450.45	2	225.23	19.76	2.13
e				11.40	9	1.27	0.11	0.11
T	2444.30	2248.3	2000.60	20991.96	17			100

Note: *SS* is the sum of square, *v* is the degrees of freedom, *V* is the variance, *F* is the Fisher's ratio, *P* is the percentage of contribution and *T* is the sum squares due to total variation.

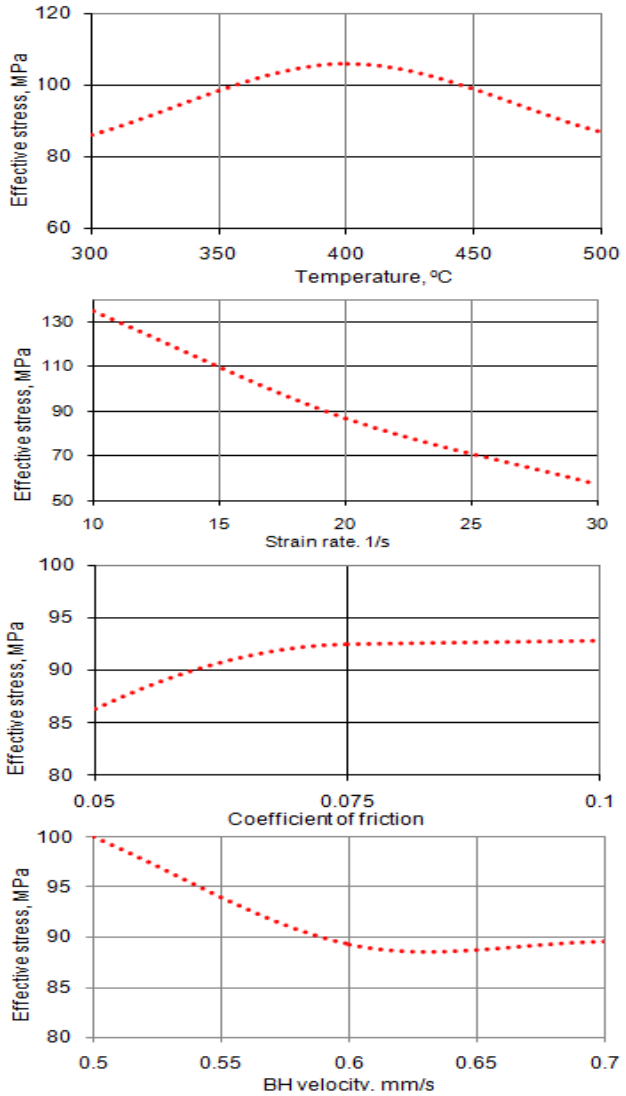

Fig-2: Influence of process parameters: (a) temperature, (b) strain rate, (c) coefficient of friction and (d) blank holder velocity on effective stress.

The effective stress was increased with an increase of temperature from 300 to 400°C and thereafter decreased from 400 to 500°C (figure 2a). The recrystallization temperature of AA1050 is about 400°C. When the deep drawing was carried out above the recrystallization temperature the metal had reduced yield strength, also no strain hardening was occurred as the material was plastically deformed. This might be the reason for the reduction of effective stress above 400°C. In general, the flow stress increases with the increase of strain rate. Here, a different phenomenon was observed. The effective stress was decreased with the increase of strain rate (figure 2b). In every instance, the flow stress increases with increasing strain during the initial stage of deformation. However, having reached a peak value, the stress reduces as the strain is increased further. It is thought that this reduction in stress takes place when the strain and strain rate hardening effect is outweighed by the softening effect induced by the heat generated during plastic deformation. The requirement of drawing load was also decreased with the increase of strain rate and above the recrystallization temperature (figure 3). A general expression for flow stress, encompassing temperature, strain, strain rate, recrystallization has been given in the form:

$$\sigma = \frac{2}{\sqrt{3(1-m)}} K \varepsilon^n \dot{\varepsilon}^m exp(1-\beta T) \qquad (20)$$

where, *n* is strain hardening exponent, *m* is strain rate sensitivity exponent, *T* is temperature.

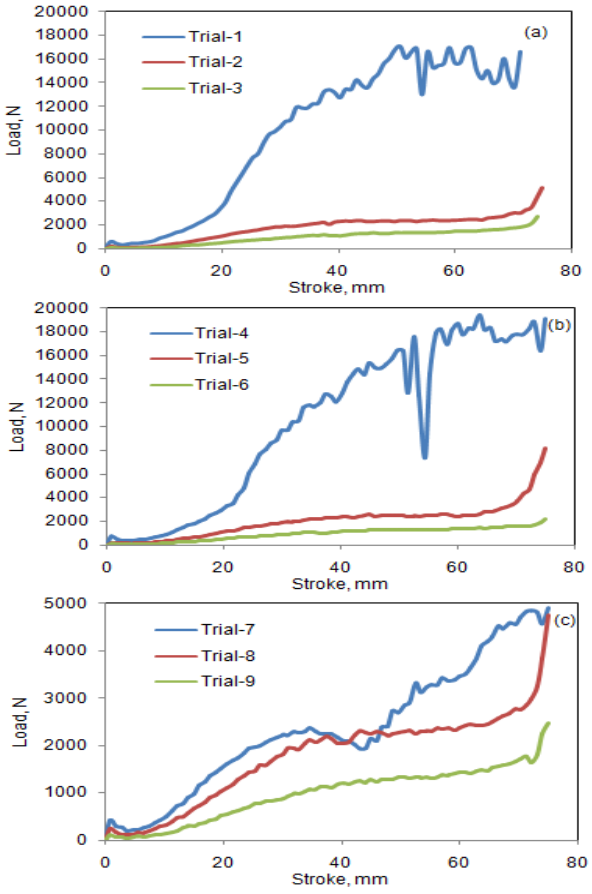

Fig-3: Influence of strain rate on load (a) at 300°C, (b) at 400°C and (c) at 500°C temperature.

The influence of friction on the effective stress is shown in figure 2c. In this work, the coefficient of friction was varied from 0.05 to 0.1.). Therefore, the shear stress due to friction would vary from 0.05P to 0.1P, where P is the normal pressure according the Eq. (15). The normal pressures developed in the conical cup drawn under trials 1 and 9 are shown in figure 4. The maximum normal pressure of 1630 MPa was observed for trial 4 of the deep drawing process. The increase in the nominal contact pressure would crush the surface asperities of the blank giving rise to more real contact area. Hence, the result was the requirement of high drawing pressure to draw the conical cup. The stress is defined as force/area. The denominator term would increase with an increase in thickness of the blank sheet, but this increase was dominated by the required drawing force to draw the conical cups. Therefore, the effective stress was increased with the increase of friction. The effective stress was decreased with the increase of blank holder velocity. As the blank holding force was maintained constant in this work, the contact time between the blank holder and the blank got reduced due to increased blank holder velocity. Subsequently, there would be less restraint to the plastic deformation and the metal flow into the die. As a result the effective stress was reduced with the increase of blank holder velocity (figure 2d).

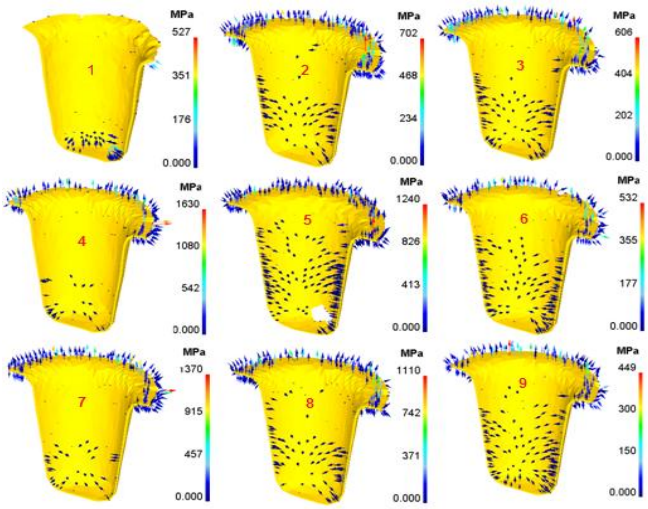

Fig-4: Normal pressures developed due to friction during deep drawing process.

The FEA results of effective stress are shown in figure 5 for various test conditions as per the design of experiments. For trials 1, 2 and 3, the temperature was 300^{o}C. The strain rates were 10, 20 and 30 s^{-1}, respectively for trails 1, 2 and3. The coefficients of friction were 0.05, 0.075 and 0.1, respectively for trials 1, 2 and 3. The blank holder velocities were 0.5, 0.6 and 0.7, respectively for trials 1, 2 and 3. The von Mises stress was decreased with the resultant increase of strain rate, the coefficient of friction and the blank holder velocity. For trials 4, 5 and 6, the temperature was 400^{o}C.The strain rates were 10, 20 and 30 s^{-1}, respectively for trails 4, 5 and 6. The coefficients of friction were 0.075, 0.1 and 0.05, respectively for trials 4, 5 and 6. The blank holder velocities were 0.7, 0.5 and 0.6, respectively for trials 4, 5 and 6. The von Mises stress for trial 4 was higher than that of trial1due to superseding effect of the temperature and friction over the blank holder velocity. The von Mises stress for trial 5 was higher than that of trial 2 due to combined effect of the temperature, friction and blank holder velocity. The von Mises stress for trial 6 was higher than that of trial 3 due to dominant effect of the temperature and blank holder velocity over the friction. For trials 7, 8 and 9, the temperature was 500^{o}C.The strain rates were 10, 20 and 30 s^{-1}, respectively for trails 7, 8 and 9. The coefficients of friction were 0.1, 0.05 &0.075, respectively for trials 7, 8 & 9. The blank holder velocities were 0.6, 0.7 and 0.5, respectively for trials 7, 8 and 9. The von Mises stress for trial 7, 8 and 9 were lower than that of trial 4, 5 & 6 respectively and higher than that of trial 1, 2 and 3 respectively.

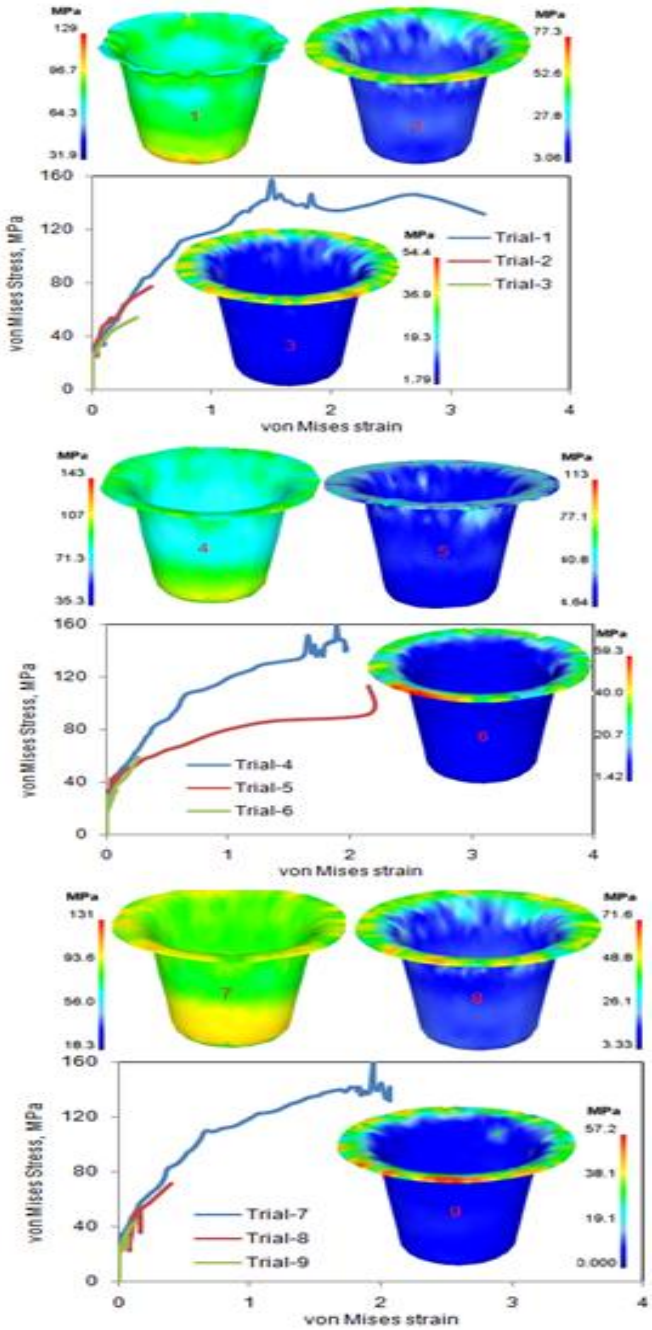

Fig-5: Effect of process parameters on the effective stress.

4.2 Influence of Process Parameters on Surface Expansion Ratio

The material formability is an evaluation of how much deformation a material can undergo before failure. In the deep drawing process the plastic deformation in the surface is much more pronounced than in the thickness. The author introduces the term surface expansion ratio to measure the formability of cups. This depicts the formability and ductility of the blank material drawn into the cup.

$$\text{Surface expansion ratio} = \frac{A_i}{A_0} \quad (21)$$

where, A_i is the instantaneous surface area of the cup drawn and A_0 is the initial blank surface area.

Table-4: ANOVA summary of the surface expansion ratio

Source	Sum 1	Sum 2	Sum 3	*SS*	*v*	*V*	*F*	*P*
A	11.74	12.86	11.65	0.15	2	0.08	1.89	18.24
B	10.74	12.76	12.75	0.45	2	0.23	5.44	54.72
C	12.75	11.73	11.77	0.11	2	0.05	1.18	13.38
D	12.06	12.56	11.63	0.07	2	0.03	0.71	8.51
e				0.0423	9	0	0.00	5.15
T	47.29	49.91	47.8	0.8223	17			100

The ANOVA summary of surface expansion ratio is given in table 4. As per the Fisher's test (F = 3.01), the strain rate (B) all by itself would contribute the most (54.72%) towards the variation observed in the surface expansion ratio. The other process parameters were insignificant.

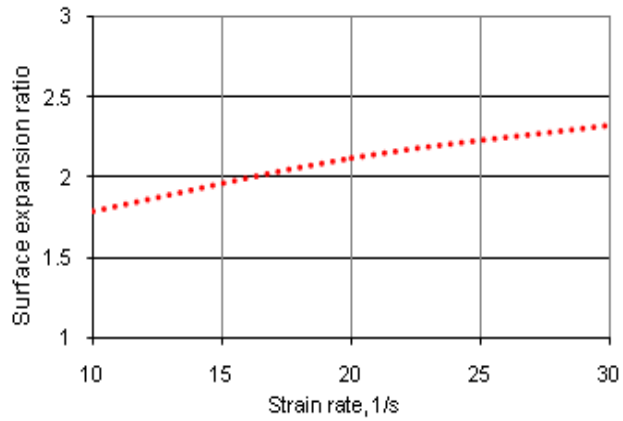

Fig-6: Effect of process parameters on the surface expansion ratio.

The surface expansion ratio would increase with an increase in the strain rate (figure 6). In the forming processes, the volume of the material remains constant before and after the forming process. On account of the punch force, the blank material undergoes plastic deformation to form the cup. As the plastic deformation is irreversible, the cup retains its shape. Experimentally, it has been observed that the surface area of the cup drawn is always higher than the initial blank surface area [8]. The value of the stress at an arbitrary time point would only depend on the current values of strain, strain rate and temperature. A sudden change of strain rate from $\dot{\varepsilon}1$ to $\dot{\varepsilon}_2$ would lead to a corresponding increase of stress from σ_1 to σ_2. After each sudden change of $\dot{\varepsilon}$, a stress transient was observed. Depending on the previous deformation history, the stress may be at first either higher or lower than the expected value. This phenomenon represents the microstructural state and can be determined in terms of structural change during the deformation process [1]. The deformation of grain boundary towards the tensile direction would contribute more to the total elongation, as the strain rate increases; this can be the most possible reason for the increase of surface expansion ratio with an increase in the strain-rate.

In the thermally activated deformation process, the thermal energy is distributed between the processes of superplastic flow and grain growth [1]. The microstructure of AA1050 as detected before (figure 7a) and after (figure 7b) deep drawing process reveals grain sliding and elongation in the direction of tensile loading. The phenomenon of grain growth in the superplastic deformation is accompanied by grain boundary sliding as shown in figure 8. The initial length of hexagonal array is L (figure 8a). After diffusional deformation the length of array is) L+ΔL(d) as shown in figure 8b. The dark regions represent separation between the grains (figure 8b,). After grain boundary sliding, the length of array is L+ΔL(d)+ +ΔL(s) as shown in figure 8c [13].

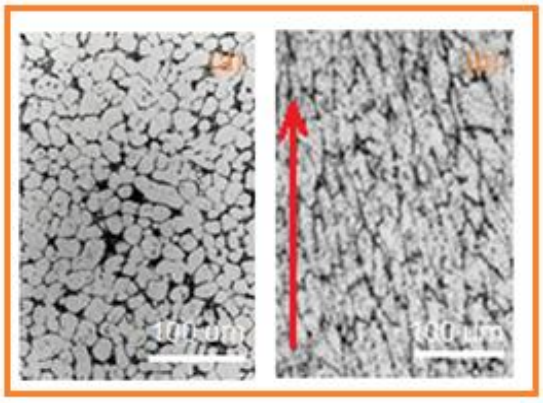

Fig-7: Microstructure AA1050 (a) before deep drawing (b) after deep drawing.

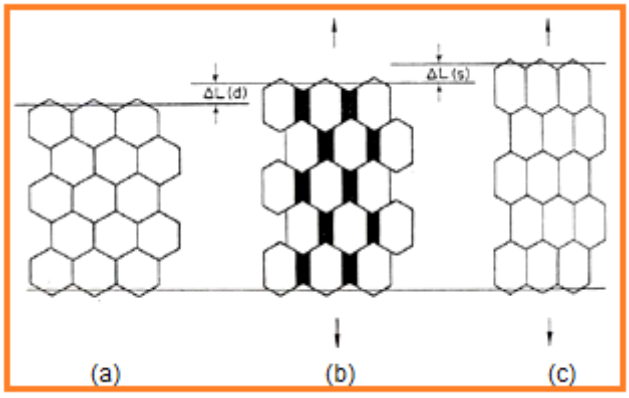

Fig-8: Diffusional deformation and grain boundary sliding of an array of hexagonal grains.

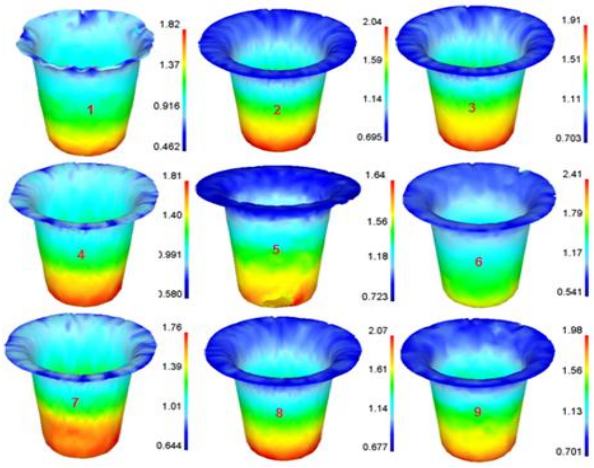

Fig-9: Influence of process parameters on the surface expansion ratio.

The FEA results of surface expansion ratio are revealed in figure 9 for various test conditions as per the design of experiments. For the surface expansion ratio greater than 2.0 the height of the cups was between 76.2 to 76.7 mm for the trials 2, 6 and 8. For the remaining trails the surface expansion ratios were lower than 2.0 yielding the cup height in the range of 75.2 to 76 mm (figure 10).

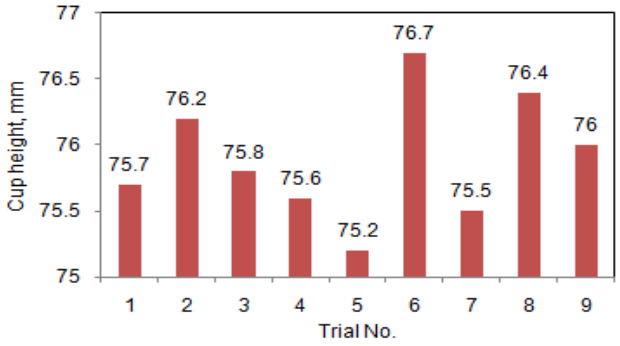

Fig-10: Cup heights under different trials.

4.4 Influence of Process Parameters on Damage of Cup

The ANOVA summary of damage of cups is given in table 5. When the Fisher's test (3.01) was applied to ascertain the influence of process parameters it was found that the temperature (A), strain rate (B), the coefficient of friction (C) and the blank holder velocity (D), respectively had contributed 5.70%), 83.41%, 6.33% and 4.27% of the total variation in the cups heights drawn.

Table-5: ANOVA summary of damage of the cups

Source	Sum 1	Sum 2	Sum 3	*SS*	*v*	*V*	*F*	*P*
A	3.16	4.15	5.25	0.36	2	0.18	9.80	5.70
B	8.76	1.50	2.30	5.27	2	2.64	143.68	83.41
C	2.98	5.10	4.48	0.40	2	0.20	10.88	6.33
D	5.23	3.68	3.64	0.27	2	0.14	7.62	4.27
e				0.02	9	0.00	0.00	0.29
T	20.12	14.43	15.68	6.32	17			100

The damage factor in the cups is defined as follows:

$$D_f = \int \frac{\sigma_1}{\sigma_{es}} d\varepsilon \qquad (22)$$

where, σ_1 is the tensile maximum principal stress; σ_{es} is the effective stress; and $d\varepsilon$ is the effective strain increment.

The damage in the conical cups was increased with an increase in the temperature and the coefficient of friction (figure 11a & 11c). The damage was decreased with the strain rate and the blank holder velocity (figure 11b & 11d). The folding of sheet was happened with the combination of low friction coefficient; whereas there was no or less folding with the high coefficient of friction. In the case of friction between the blank and the tool, the increase of the coefficient of friction determines the wrinkling to reduce, but high values of the friction coefficient may cause cracks and material breakage [14]. The wrinkling was observed in the cup drawn by means of trial 1 with the coefficient of friction of 0.05. This was experimentally validated. The damage was found in the cup drawn under trial 5 with the coefficient of friction of 0.1 (figure 13).

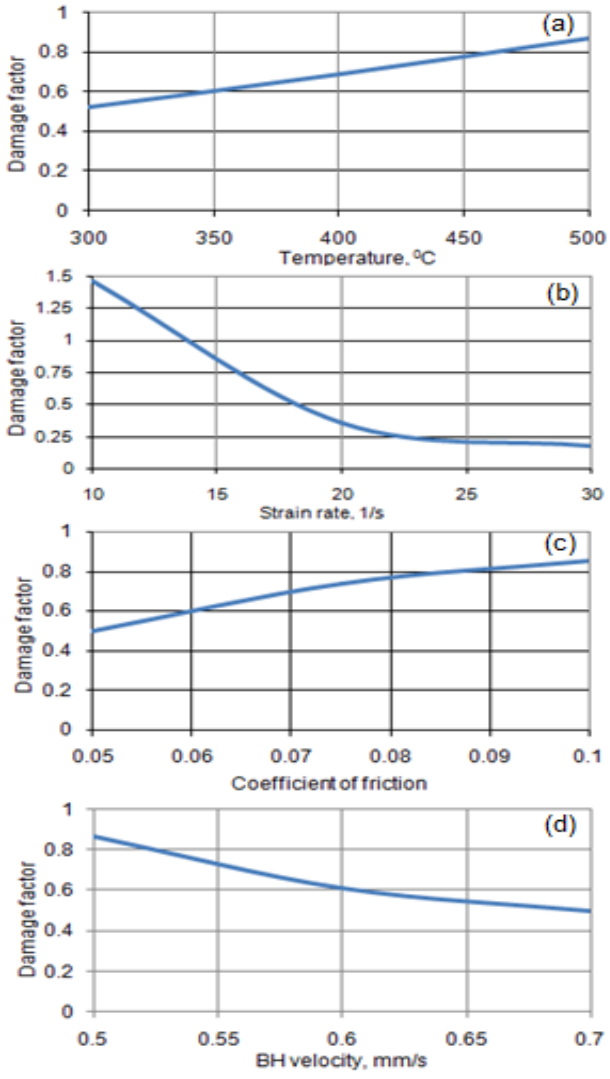

Fig-11: Influence of process parameters on the damage of cup.

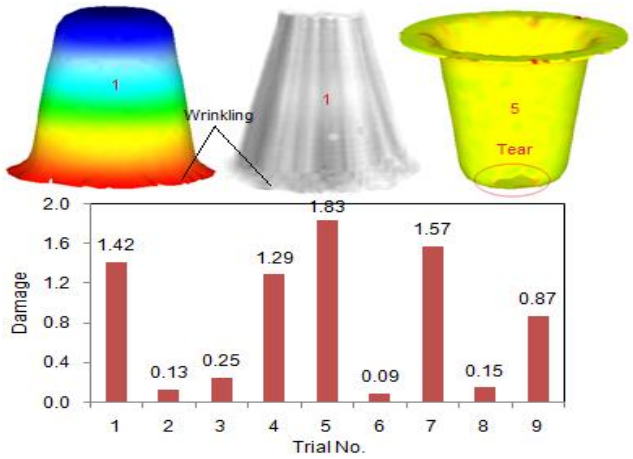

Fig-12: Damages in the cups.

Figure 13 depicts the forming limit diagram (FLD) with damages in the conical cups drawn from AA1050-H18 sheets at temperature 300°C. The first branch covers the range from equal bi-axial tension to plain strain. The second branch corresponds to plain strain and uniaxial tension. The third branch extends from uniaxial tension to pure shear. The fourth branch widens from pure shear to uniaxial compression. The FLD for the conical cup drawn by means of trial 1 is in the fourth branch. The conical cup drawn using trial 1 had wrinkles as the minor strain was twice the major strain induced in the blank material. The slits were observed in the cups drawn by means of trials 2 and 3 due to shear in the flange area of the blank material. Figure 14 represents the forming limit diagram (FLD) with damages in the conical cups drawn from AA1050-H18 sheets at temperature 400°C. The FLD for the conical cup drawn using trial 4 is in the fourth branch. The conical cup drawn by trial 4 had wrinkles. Necking of the blank sheet took place near the punch profile due to excess tensile stress, resulting in fracture in the cup drawn under trial 5. Figure 15 characterizes the forming limit diagram (FLD) with damages in the conical cups drawn from AA1050-H18 sheets at temperature 500°C. The conical cups drawn by trial 7 were worn out in the near the punch profile due to equal biaxial tension. The wrinkles were observed in the flange area for the cups drawn using trials 7 and 9. The shabby marks were observed in the flange area of the cup drawn under trial 8 due to excessive shear stress.

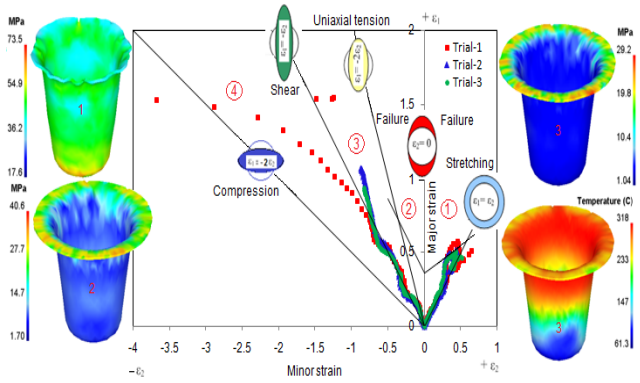

Fig-13: Forming limit diagram with damage in the cups drawn at temperature 300°C.

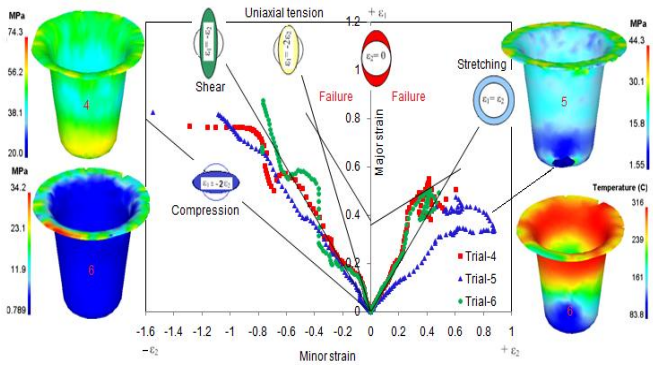

Fig-14: Forming limit diagram with damage in the cups drawn at temperature 400°C.

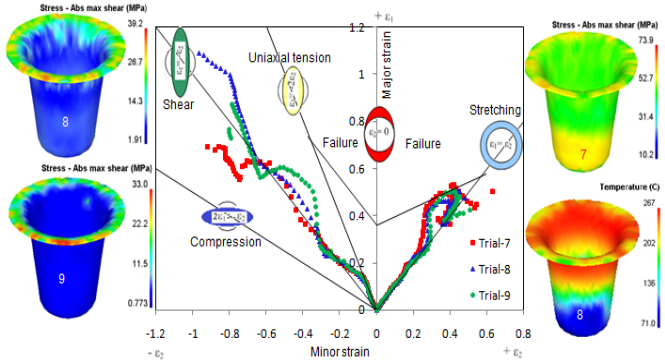

Fig-15: Forming limit diagram with damage in the cups drawn at temperature 500°C.

5. CONCLUSION

The strain rate by itself has a sizeable effect on the effective stress and the height of the conical cup drawn. With the increase of temperature the cup material becomes soft and thereby the stress induced in the cup material decreases due to reduction of the drawing force. For the surface expansion ratio greater than 2.0 the height of the cups is between 76.2 to 76.7 mm. The wrinkling was observed in the conical cups drawn with the low coefficient of friction; whereas necking was noticed with the high coefficient of friction.

ACKNOWLEDGMENTS

The author wishes to thank University Grants Commission (UGC), New Delhi, India for financial assisting this project.

REFERENCES

[1]. A. Chennakesava Reddy, Finite element analysis of reverse superplastic blow forming of Ti-Al-4V alloy for optimized control of thickness variation using ABAQUS, Journal of Manufacturing Engineering, 2006, 1(1), pp.06-09.
[2]. T. Srinivas and A.C. Reddy, Parametric Optimization of Warm Deep Drawing Process of 1100 Aluminum Alloy: Validation through FEA, International Journal of Scientific & Engineering Research, 2015, 6(4), pp.425-433.
[3]. B. Yamuna and A.C. Reddy, Parametric Merit of Warm Deep Drawing Process for 1080A Aluminium Alloy: Validation through FEA, International Journal of Scientific & Engineering Research, 2015, 6(4), pp.416-424.

[4]. K. Chandini and A.C. Reddy, Parametric Importance of Warm Deep Drawing Process for 1070A Aluminium Alloy: Validation through FEA, International Journal of Scientific & Engineering Research, 2015, 6(4), pp.399-407.
[5]. H. Takuda, K. Mori, I. Masuda, Y. Abe and M. Matsuo, Finite element simulation of warm deep drawing of aluminum alloy sheet when accounting for heat conduction, Journal of Materials Processing Technology, 2002, 120, pp.412–418.
[6]. K.P. Rao, Y. K. D. V. Prasad and E. B. Hawbolt, Hot deformation studies on a low – carbon steel: Part I – Flow curves and the constitutive relationship, Journal of materials processing technology, 1996, 56, pp.897–907.
[7]. A. Chennakesava Reddy, T. Kishen Kumar Reddy and M. Vidya Sagar, Experimental characterization of warm deep drawing process for EDD steel, International Journal of Multidisciplinary Research & Advances in Engineering, 2012, 4, pp.53-62.
[8]. A. Chennakesava Reddy, Evaluation of local thinning during cup drawing of gas cylinder steel using isotropic criteria, International Journal of Engineering and Materials Sciences, 2012, .5, pp.71-76.
[9]. F. Shehata, M. J. Painter and R. Pearce, Warm forming of aluminum/magnesium alloy sheet, Journal of Mechanical Working Technology, 1978, 2, pp.279-291.
[10]. Chennakesava R Alavala, CAD/CAM: Concepts and Applications, PHI Learning Solutions Private Limited, New Delhi, 2007.
[11]. Chennakesava R Alavala, Finite Element Methods: Basic Concepts and Applications, PHI Learning Solutions Private Limited, New Delhi, 2008.
[12]. G. R. Johnson and W. H. Cook, A constitutive model and data for metals subjected to large strains, high strain rates and high temperatures, In Proceedings of the Seventh Symposium on Ballistics, The Hague, The Netherlands, 1983, pp.1-7.
[13]. W.R.Cannon, The contribution of grain boundary sliding to axial strain during diffusion creep, Philosophical Magazine, 1972, 25(6), p1489-1497.
[14]. J. Hedworth and M.J. Stowell, The measurement of strain-rate sensitivity in superplastic alloys, Journal of Material Science, 1971, 6, pp.1061–1069.

BIOGRAPHY

Dr. A. Chennakesava Reddy, B.E., M.E (prod). M.Tech (CAD/CAM)., Ph.D (prod)., Ph.D (CAD/CAM) is a Professor in Mechanical Engineering, Jawaharlal Nehru Technological University, Hyderabad. The author has published 252 technical papers worldwide. He is the recipient of best paper awards nine times. He is recipient of Best Teacher Award from the Telangana State, India. He has successfully completed several R&D and consultancy projects. He has guided 14 Research Scholars for their Ph.D. He is a Governing Body Member for several Engineering Colleges in Telangana. He is also editorial member of Journal of Manufacturing Engineering. He is author of books namely: FEA, Computer Graphics, CAD/CAM, Fuzzy Logic and Neural Networks, and Instrumentation and Controls. Number of citations are 518. The total impact factors are 136.938. The author's h-index and i10-index are 18 and 21 respectively. His research interests include Fuzzy Logic, Neural Networks, Genetic Algorithms, Finite Element Methods, CAD/CAM, Robotics and Characterization of Composite Materials and Manufacturing Technologies.